Communication

Sapphire-Derived Fiber Bragg Gratings for High Temperature Sensing

Qi Guo [1], Zhixu Jia [1], Xuepeng Pan [1], Shanren Liu [1], Zhennan Tian [1], Zhongming Zheng [2], Chao Chen [2], Guanshi Qin [1] and Yongsen Yu [1,*]

[1] State Key Laboratory of Integrated Optoelectronics, College of Electronic Science and Engineering, Jilin University, Changchun 130012, China; qiguo18@mails.jlu.edu.cn (Q.G.); jiazx@jlu.edu.cn (Z.J.); panxp20@mails.jlu.edu.cn (X.P.); liusr19@mails.jlu.edu.cn (S.L.); zhennan_tian@jlu.edu.cn (Z.T.); qings@jlu.edu.cn (G.Q.)

[2] Changchun Institute of Optics, Fine Mechanics and Physics, Chinese Academy of Sciences, Changchun 130033, China; zhengzm@ciomp.ac.cn (Z.Z.); chenc@ciomp.ac.cn (C.C.)

* Correspondence: yuys@jlu.edu.cn

Abstract: In this paper, a sapphire-derived fiber (SDF) with a core diameter of 10 µm and a cladding diameter of 125 µm is fabricated by the melt-in-tube method, and fiber Bragg gratings (FBGs) with reflectivity over 80% are prepared by the femtosecond laser point-by-point direct writing method. By analyzing the refractive index distribution and reflection spectral characteristics of the SDF, it can be seen that the SDF is a graded refractive index few-mode fiber. In order to study the element composition of the SDF core, the end-face element distribution of the SDF is analyzed, which indicates that element diffusion occurred between the core and the cladding materials. The temperature and stress of the SDF gratings are measured and the highest temperature is tested to 1000 °C. The temperature and strain sensitivities are 15.64 pm/°C and 1.33 pm/µε, respectively, which are higher than the temperature sensitivity of the quartz single-mode fiber. As a kind of special fiber, the SDF expands the application range of sapphire fiber, and has important applications in the fields of high-temperature sensing and high-power lasers.

Keywords: sapphire-derived fiber (SDF); melt-in-tube method; fiber Bragg gratings (FBGs); femtosecond laser

1. Introduction

Optical fiber sensors have important applications in monitoring extreme environmental conditions, such as high temperature, high pressure, strong radiation, and strong electromagnetic interference [1–3], and most of them use standard quartz single-mode optical fibers. Limited by the existing low-concentration doped optical fiber, the stability and mechanical strength of optical fiber devices will deteriorate at higher temperatures [4], which seriously restricts the application of optical fiber sensors. Therefore, it is necessary to explore and develop a high-temperature optical fiber with good mechanical properties in order to achieve a new breakthrough in high-temperature optical fiber sensing.

Single crystal sapphire fiber sensors have always been considered the preferred solution in the field of high-temperature sensing. However, because sapphire fiber has no cladding and is highly multimodal [5,6], sensor packaging and signal demodulation are also difficult. For the traditional quartz fiber laser, the further increase in power is mainly limited by the damage threshold and stimulated Brillouin scattering [7]. Therefore, choosing a material with better thermal performance and smaller Brillouin scattering coefficient as the gain medium of a fiber laser is an effective way to break the current power limitation of fiber laser and obtain higher output power. In 2012, John Ballato et al. from Clemson University proposed and drew sapphire-derived fiber (SDF) for the first time [7]. This kind of optical fiber is a special optical fiber drawn by a single crystal sapphire rod as the core

rod and a quartz tube as the sleeve under high-temperature conditions [7]. In the process of high-temperature drawing, the fused sapphire diffuses with the fused quartz material to form a high concentration of alumina-doped alumina glass core [8]. By controlling the parameters of the drawing process, the doping concentration can be adjusted and the Brillouin gain coefficient can be controlled. Researchers have measured the lowest Brillouin gain coefficient in the current fibers, and it is also a temperature-independent Brillouin frequency fiber, which is a Brillouin athermal optical fiber.

In recent years, Pang et al. discovered that when SDF is arc-discharged, mullite crystals will precipitate in the local area of highly doped fiber core. By using this crystallization effect, the refractive index of the fiber core can be modulated, and the highest refractive index modulation can reach 0.015. Based on the principle of discharge crystallization, they prepared a SDF Fabry–Perot (F-P) interference sensor [9,10], a Mach–Zendel (M-Z) interference sensor [11], and a long period grating sensor [12], which expanded the application range of SDFs.

Fiber Bragg gratings (FBGs) have important applications in the field of optical fiber sensing. Generally, FBGs can be prepared in different types of optical fibers by the phase mask method and the femtosecond laser direct writing method [13–15]. The femtosecond laser direct writing method has good flexibility and can be used to fabricate gratings of different periods and types [16–18]. At the same time, a femtosecond laser has an ultra-short pulse duration and ultra-high peak power [19–21]. Based on the principle of multi-photon absorption, it can realize the refractive index modulation of different amplitudes inside the transparent material [22,23] and can realize ultra-fine cold processing. Therefore, high-temperature resistant fiber gratings can be prepared by femtosecond laser-induced permanent refractive index changes in different kinds of fibers, which has important application value in the field of high-temperature fiber sensing [24,25]. In 2014, Tino Elsmann et al. successfully prepared a SDF with a core diameter of 21 μm and a cladding diameter of 125 μm, and prepared FBGs using a two-beam phase mask interferometer system [4]. Because the SDF is drawn by a large-diameter sapphire rod and a quartz tube, the core diameter is large and the reflection spectrum is highly multimodal. It needs to be tested by multimode fiber coupling, and the spectral bandwidth will increase, which is not conducive to high-resolution demodulation.

In this paper, a SDF with a core diameter of 10 μm and a cladding diameter of 125 μm is fabricated by the melt-in-tube method. The core and cladding diameter of this SDF are similar to that of a single-mode fiber, and the spectrum can be tested by single-mode fiber coupling, which improves the demodulation accuracy of the system. In addition, the 515-nm femtosecond laser direct writing system combined with point-by-point method is used to realize the preparation of FBGs. The end-face element distribution of the SDF is tested and analyzed by an energy dispersive spectrometer (EDS). The high-temperature and strain-sensing characteristics of the prepared gratings are studied, and the temperature sensitivity obtained is higher than that of quartz single-mode fiber. The SDF has good temperature stability and high temperature resistance, and can be applied in the field of high-temperature sensing.

2. Preparation and Characterization of SDF

The SDF was prepared by the melt-in-tube method. A single crystal sapphire rod was used as the core rod of preform rod, and a quartz tube was used as the sleeve. The special optical fiber was prepared by a fiber-drawing tower at high temperature. Figure 1a shows the preparation process of the SDF preform rod. The core rod was a single crystal sapphire rod with a diameter of 450 μm, and the sleeve was a quartz tube with an inner diameter of 500 μm and outer diameter of 10 mm. Figure 1b presents the schematic diagram of the SDF fabricated by the melt-in-tube method. The preform rod was placed in the fiber-drawing tower, heated by graphite furnace, and the drawing temperature was about 2100 °C. The drawing speed was accurately controlled by program and motor, and the diameter of SDF

was measured in real time by a laser diameter-measuring instrument. Figure 1c,d shows photos of the fiber preform rods before and after drawing.
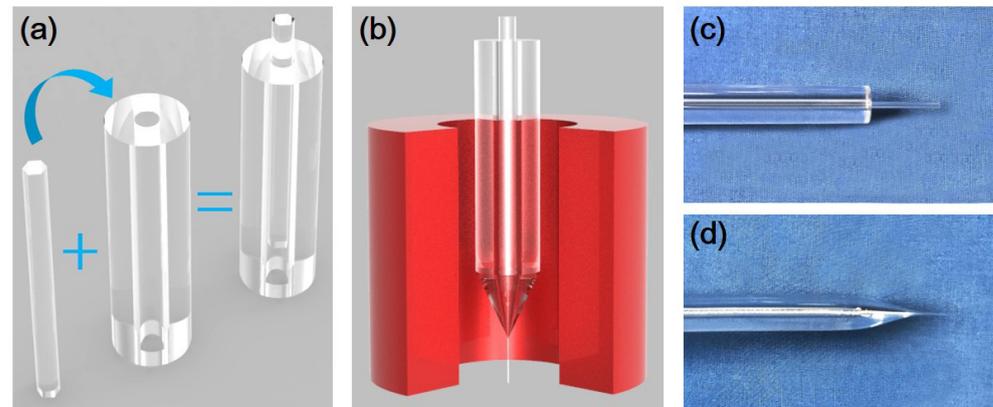
Figure 1. Fabrication of a sapphire-derived fiber (SDF) by the melt-in-tube method. (**a**) Preparation process of the fiber preform based on sapphire crystal. (**b**) Diagram of the SDF drawing process; (**c,d**) shows the photos of the fiber preform rods before and after drawing.

Figure 2a shows the micrograph of the end face of the SDF prepared by the melt-in-tube method. The core diameter is about 10 μm and the cladding diameter is about 125 μm. This is close to the size of a standard single-mode fiber. In addition, since the cladding material is quartz, it can be fused by optical fiber fusion splicer, which is very compatible with quartz optical fiber. The end-face refractive index distribution of the SDF was measured by a fiber end-face refractive index analyzer (SHR-1802, China), and the wavelength of the test light was 633 nm. The end-face refractive index distribution is shown in Figure 2b, and the refractive index difference between the core and the cladding is about 0.06.
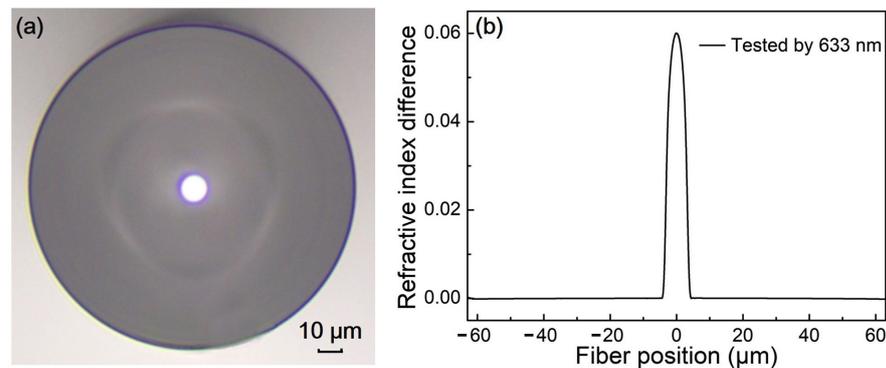
Figure 2. (**a**) Micrograph of the SDF end face. (**b**) Refractive index profile of the SDF.

The elements in the SDF core area were tested and analyzed by an EDS, which is produced by EDAX TEAM company of America. In the EDS surface scanning results (shown in Figure 3a), we can see that oxygen, aluminum, and silicon are all present in the core. Oxygen is uniformly distributed, and aluminum is mainly distributed in the core. In the EDS line scanning results of core position (shown in Figure 3b,c), we can see that the content of silicon gradually decreases from both sides to the middle, while the content of aluminum element gradually decreases from the center to both sides, and the distribution of the two elements is parabolic. The core also contains silicon, and the content of silicon in the cladding is obviously higher than that in the core, which indicates that during the high-temperature drawing process, the sapphire single crystal melts, and the core and cladding materials diffuse, so that aluminum and silicon are in a transitional distribution state in the core.
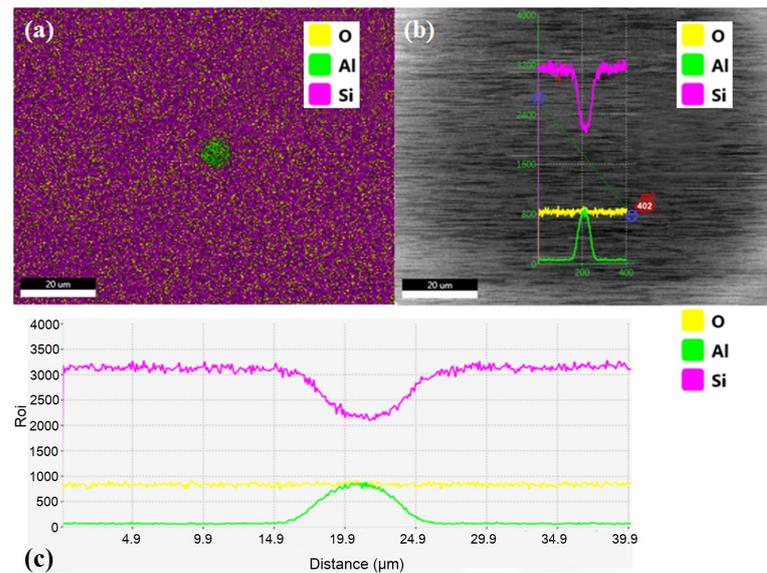
Figure 3. (**a**) The element distribution of SDF characterized by energy dispersive spectrometer (EDS) surface scanning. (**b**,**c**) The element distribution of SDF characterized by EDS line scanning.

3. Design Results and Discussion

3.1. FBGs Prepared in SDF

The device for preparing FBGs by the femtosecond laser point-by-point method is shown in Figure 4a. The femtosecond laser (Light-Conversion Pharos, Lithuania) was used with a working wavelength of 1030 nm, repetition frequency of 200 kHz, and pulse width of 290 fs. A frequency doubling crystal (β-BaB$_2$O$_4$) (BBO) was used to double the frequency of the 1030-nm laser emitted by the laser to obtain a 515 nm laser. A shorter laser wavelength is conducive to the realization of finer processing. The 515-nm laser was focused into the center of the SDF core through an oil immersion objective lens (Olympus, 60×/1.42, Japan), and FBGs were prepared by the point-by-point method.
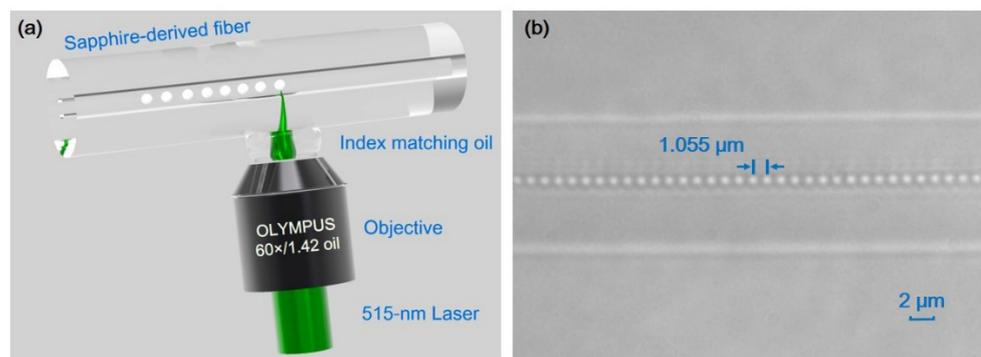
Figure 4. (**a**) Schematic diagram of the fiber Bragg grating (FBG) prepared in SDF by point-by-point method. (**b**) The micrograph of the prepared FBG.

The FBGs were fabricated in the SDF by using a 515-nm femtosecond laser processing system. Figure 4b presents a photomicrograph of the FBG prepared in the SDF. Since the SDF cladding was made of quartz material, the SDF and quartz optical fiber could be fused together by a fusion splicer to achieve high coupling efficiency. The spectrum of the SDF was measured by an optical spectrum analyzer (OSA) (Yokogawa AQ6370D, Japan), supercontinuum light source (NKT Photonics, Denmark), and single-mode fiber

coupler. Figure 5 shows the reflection and transmission spectra of the prepared FBG. The FBG phase-matching condition is given by the following formula [26]:

$$m\lambda_B = 2n_{eff}\Lambda \tag{1}$$

where *m* is the grating order, λ_B is the wavelength, n_{eff} is the effective refractive index, and Λ is the grating period. The prepared grating order is *m* = 2, the grating period is 1.055 μm, the central wavelength of the peak with the maximum reflectivity in the reflection spectrum is 1549.56 nm, the reflectivity is more than 80%, the full width at half maximum (FWHM) is 0.3298 nm, and the side-mode suppression ratio (SMSR) is 10 dB. It can be calculated that the refractive index of the core is about 1.4688 (@1550 nm). It can be seen from the transmission spectrum that there is some insertion loss in the prepared device. This is due to the mismatch of mode field diameter between the SDF and quartz single-mode fiber, and the waveguide defects caused by the preparation of high reflectivity gratings, which lead to scattering loss. In addition, the core material of the SDF is different from that of the quartz fiber, which leads to end-face Fresnel reflection loss when splicing at the interface. There are three reflection peaks in the reflection spectrum, which is mainly due to the large refractive index difference between the core and cladding of the SDF. Although the diameter of the core and cladding is close to the parameters of a single-mode fiber, it still has the characteristics of a few-mode fiber. It can be seen from the refractive index distribution of the fiber end face and the spectral test results that this SDF is a few-mode fiber with graded refractive index distribution.
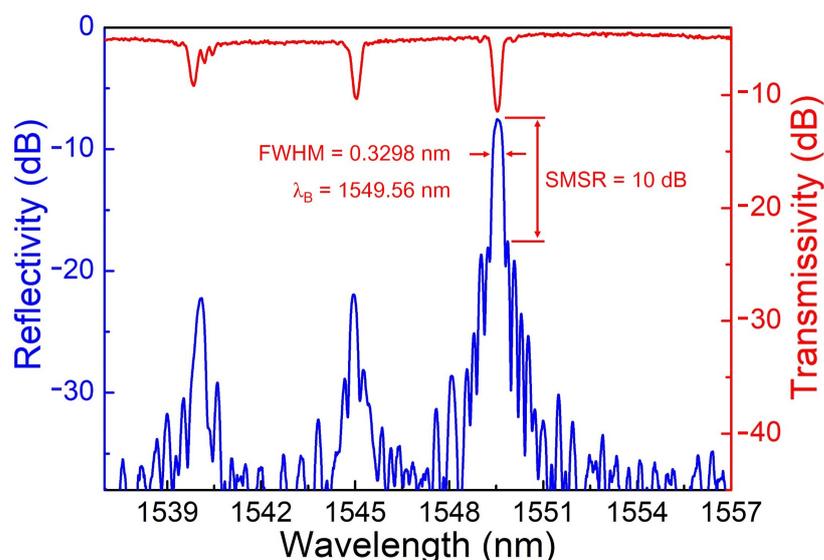
Figure 5. Reflection and transmission spectra of FBG prepared in the SDF by the point-by-point method. FWHM: full width at half maximum; SMSR: side-mode suppression ratio.

3.2. SDF Gratings Temperature Testing

In order to test the high-temperature characteristics of the SDF grating, the prepared FBG was put into a muffle furnace, heated to 1000 °C for 2 h, and then cooled to room temperature. This annealing process was used in order to eliminate the unstable structure and residual stress during the preparation of FBGs by femtosecond laser. Next, the FBG was tested from room temperature to 1000 °C and the temperature test interval was 100 °C. Each temperature point was kept for 30 min, and 11 temperature points were tested. Figure 6 shows the drift curve of the resonant wavelength of the SDF grating with the change of temperature and shows the red shift characteristic.
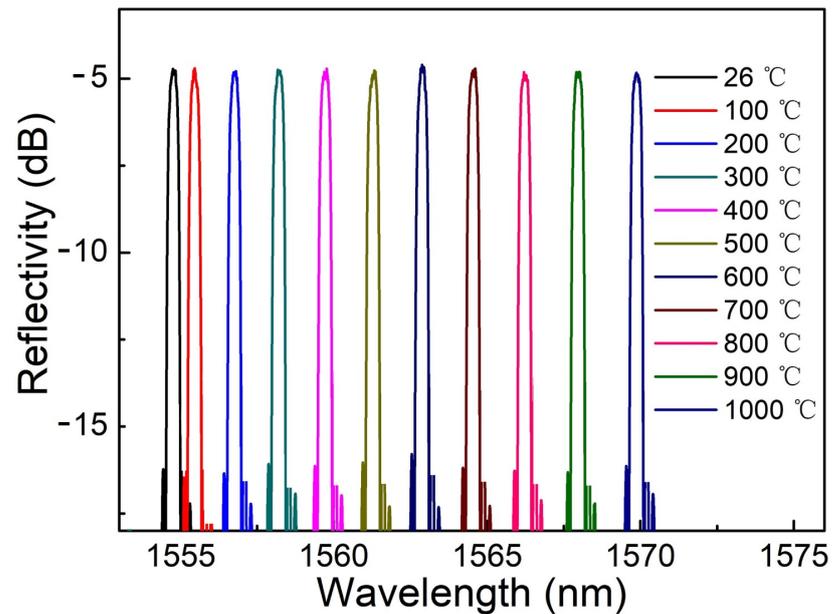
Figure 6. The reflection spectrum varies with temperature from room temperature to 1000 °C.

Figure 7 shows the fitting curve of the wavelength shift and temperature change of the SDF grating. The temperature sensitivity obtained by linear fitting is 15.64 pm/°C. A better fitting effect was obtained through quadratic fitting; the fitting similarity is 0.9997, and the quadratic fitting function is shown as follows:

$$Y = 3.41556 \times 10^{-6} X^2 + 0.01217 X + 1554.29567 \tag{2}$$
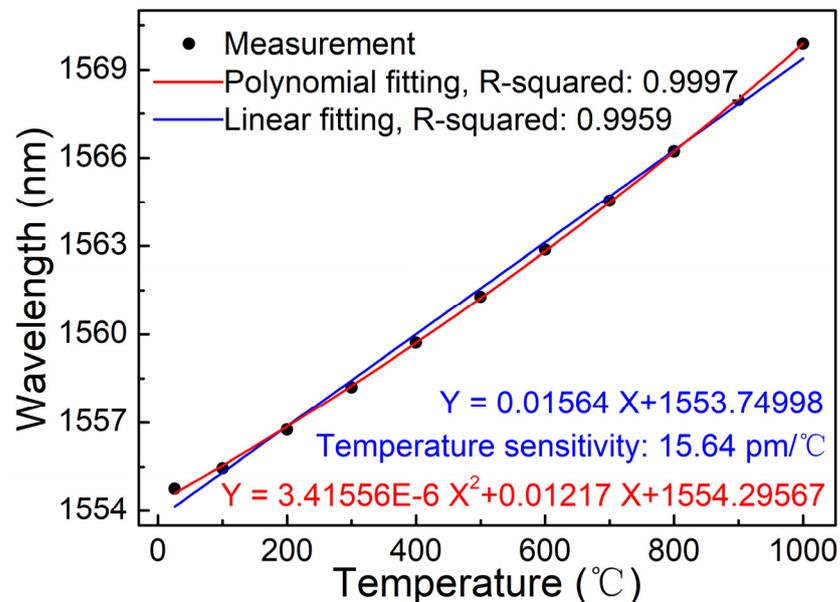
Figure 7. Polynomial fitting and linear fitting relationship between resonance wavelength and temperature.

3.3. SDF Gratings Strain Testing

The SDF grating was fixed to the stress-testing device (WDW-100, China); the maximum stress was 1 N, and the test point interval was 0.1 N. The stabilized spectrum was

recorded by OSA, and Figure 8 shows the shift curve of resonance wavelength with stress and shows red shift characteristic.
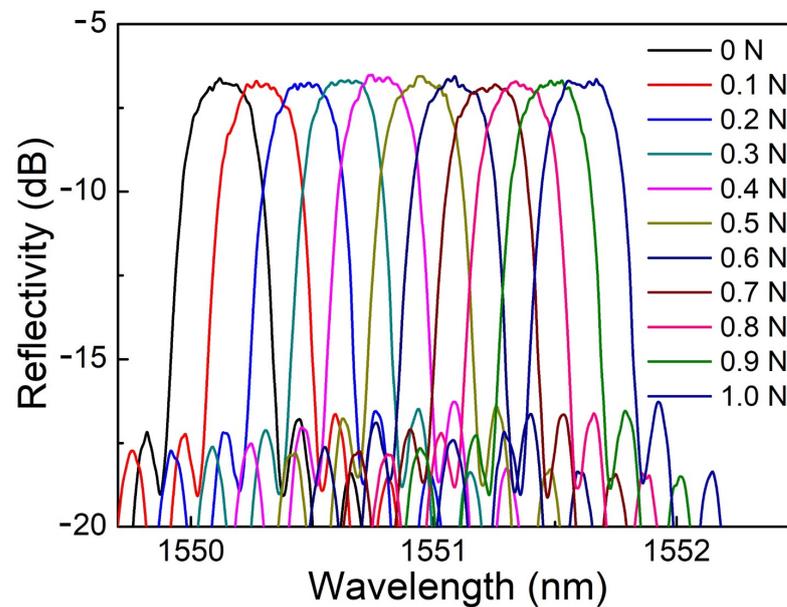
Figure 8. The reflection spectrum varies with stress.

Axial strain ε can be obtained by the following formula [27]:

$$\varepsilon = F/\pi r^2 E \tag{3}$$

where r is the fiber radius, F is the axial stress, and E is Young's modulus. Because the main component of the SDF is quartz, the Young's modulus here is approximately 73 GPa, which does not affect the calculation of strain sensitivity. The linear fitting curve of resonance wavelength and strain is shown in Figure 9, and the strain sensitivity is 1.33 pm/µε.
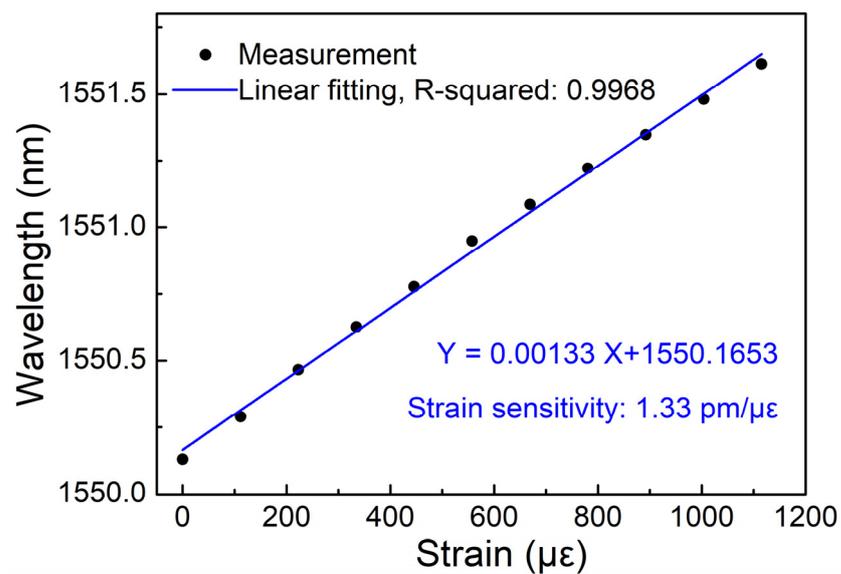
Figure 9. Linear fitting of resonance wavelength and strain.

4. Conclusions

In conclusion, a few-mode fiber SDF was successfully fabricated by the melt-in-tube method. The element distribution on the end face of the SDF was measured and analyzed

by using the surface scanning and line scanning of an EDS. The experimental results show that in the process of preparing the SDF by the melt-in-tube method, the sapphire single crystal rod melted and diffused with the fused silica material to form a high-concentration alumina-doped glass core. The temperature and strain sensitivities of the SDF gratings were 15.64 pm/°C and 1.33 pm/με, respectively, which are higher than those of a quartz single-mode fiber. The SDF demonstrated good high-temperature resistance, with the highest temperature tested at 1000 °C. The melt-in-tube method provides a convenient and direct research method for customizing optical fibers with different components. In addition, the new high-alumina content SDF has shown promise as one of the ideal transmission media for manufacturing enhanced fiber sensors and high-power fiber lasers.

References

1. Blanchet, T.; Desmarchelier, R.; Morana, A.; Boukenter, A.; Ouerdane, Y.; Marin, E.; Laffont, G.; Girard, S. Radiation and High Temperature Effects on Regenerated Fiber Bragg Grating. *J. Lightwave Technol.* **2019**, *37*, 4763–4769. [CrossRef]
2. Yang, S.; Homa, D.; Heyl, H.; Theis, L.; Beach, J.; Dudding, B.; Acord, G.; Taylor, D.; Pickrell, G.; Wang, A.B. Application of Sapphire-Fiber-Bragg-Grating-Based Multi-Point Temperature Sensor in Boilers at a Commercial Power Plant. *Sensors* **2019**, *19*, 3211. [CrossRef]
3. Zhang, Z.; He, J.; Du, B.; Zhang, F.C.; Guo, K.K.; Wang, P.P. Measurement of high pressure and high temperature using a dual-cavity Fabry-Perot interferometer created in cascade hollow-core fibers. *Opt. Lett.* **2018**, *43*, 6009–6012. [CrossRef]
4. Elsmann, T.; Lorenz, A.; Yazd, N.S.; Habisreuther, T.; Dellith, J.; Schwuchow, A.; Bierlich, J.; Schuster, K.; Rothhardt, M.; Kido, L.; et al. High temperature sensing with fiber Bragg gratings in sapphire-derived all-glass optical fibers. *Opt. Express* **2014**, *22*, 26831–26839. [CrossRef]
5. Yang, S.; Hu, D.; Wang, A.B. Point-by-point fabrication and characterization of sapphire fiber Bragg gratings. *Opt. Lett.* **2017**, *42*, 4219–4222. [CrossRef]
6. Yang, S.; Homa, D.; Pickrell, G.; Wang, A.B. Fiber Bragg grating fabricated in micro-single-crystal sapphire fiber. *Opt. Lett.* **2018**, *43*, 62–65. [CrossRef]
7. Dragic, P.; Hawkins, T.; Foy, P.; Morris, S.; Ballato, J. Sapphire-derived all-glass optical fibres. *Nat. Photonics* **2012**, *6*, 627–633. [CrossRef]
8. Ballato, J.; Hawkins, T.; Foy, P.; Kokuoz, B.; Stolen, R.; McMillen, C.; Daw, M.; Su, Z.; Tritt, T.M.; Dubinskii, M.; et al. On the fabrication of all-glass optical fibers from crystals. *J. Appl. Phys.* **2009**, *105*, 053110. [CrossRef]
9. Wang, Z.; Liu, H.; Ma, Z.; Chen, Z.; Wang, T.; Pang, F. High temperature strain sensing with alumina ceramic derived fiber based Fabry-Perot interferometer. *Opt. Express* **2019**, *27*, 27691–27701. [CrossRef] [PubMed]
10. Liu, H.; Pang, F.; Hong, L.; Ma, Z.; Huang, L.; Wang, Z.; Wen, J.; Chen, Z.; Wang, T. Crystallization-induced refractive index modulation on sapphire-derived fiber for ultrahigh temperature sensing. *Opt. Express* **2019**, *27*, 6201–6209. [CrossRef] [PubMed]
11. Xu, J.; Liu, H.H.; Pang, F.F.; Hong, L.; Ma, Z.W.; Zhao, Z.W.; Chen, N.; Chen, Z.Y.; Wang, T.Y. Cascaded Mach-Zehnder interferometers in crystallized sapphire-derived fiber for temperature-insensitive filters. *Opt. Mater. Express* **2017**, *7*, 1406–1413. [CrossRef]
12. Hong, L.; Pang, F.F.; Liu, H.H.; Xu, J.; Chen, Z.Y.; Zhao, Z.W.; Wang, T.Y. Refractive Index Modulation by Crystallization in Sapphire-Derived Fiber. *IEEE Photonics Technol. Lett.* **2017**, *29*, 723–726. [CrossRef]

13. Mihailov, S.J.; Hnatovsky, C.; Grobnic, D. Novel Type II Bragg Grating Structures in Silica Fibers Using Femtosecond Lasers and Phase Masks. *J. Lightwave Technol.* **2019**, *37*, 2549–2556. [CrossRef]

14. Goebel, T.A.; Heusinger, M.; Kramer, R.G.; Matzdorf, C.; Imogore, T.O.; Richter, D.; Zeitner, U.D.; Nolte, S. Femtosecond inscription of semi-aperiodic multi-notch fiber Bragg gratings using a phase mask. *Opt. Express* **2020**, *28*, 35682–35694. [CrossRef] [PubMed]

15. Xu, X.Z.; He, J.; He, J.; Xu, B.J.; Chen, R.X.; Wang, Y.; Yang, Y.T.; Wang, Y.P. Efficient point-by-point Bragg grating inscription in sapphire fiber using femtosecond laser filaments. *Opt. Lett.* **2021**, *46*, 2742–2745. [CrossRef] [PubMed]

16. Pan, X.P.; Guo, Q.; Wu, Y.D.; Liu, S.R.; Wang, B.; Yu, Y.S.; Sun, H.B. Femtosecond laser inscribed chirped fiber Bragg gratings. *Opt. Lett.* **2021**, *46*, 2059–2062. [CrossRef]

17. Antipov, S.; Ams, M.; Williams, R.J.; Magi, E.; Withford, M.J.; Fuerbach, A. Direct infrared femtosecond laser inscription of chirped fiber Bragg gratings. *Opt. Express* **2016**, *24*, 30–40. [CrossRef] [PubMed]

18. Williams, R.J.; Kramer, R.G.; Nolte, S.; Withford, M.J.; Steel, M.J. Detuning in apodized point-by-point fiber Bragg gratings: Insights into the grating morphology. *Opt. Express* **2013**, *21*, 26854–26867. [CrossRef] [PubMed]

19. Li, Z.Z.; Wang, L.; Fan, H.; Yu, Y.H.; Sun, H.B.; Juodkazis, S.; Chen, Q.D. O-FIB: Far-field-induced near-field breakdown for direct nanowriting in an atmospheric environment. *Light Sci. Appl.* **2020**, *9*, 41. [CrossRef] [PubMed]

20. Wang, L.; Chen, Q.D.; Cao, X.W.; Buividas, R.; Wang, X.W.; Juodkazis, S.; Sun, H.B. Plasmonic nano-printing: Large-area nanoscale energy deposition for efficient surface texturing. *Light Sci. Appl.* **2017**, *6*, e17112. [CrossRef]

21. Salter, P.S.; Booth, M.J. Adaptive optics in laser processing. *Light Sci. Appl.* **2019**, *8*, 110. [CrossRef] [PubMed]

22. Thomas, J.; Voigtlander, C.; Becker, R.G.; Richter, D.; Tunnermann, A.; Nolte, S. Femtosecond pulse written fiber gratings: A new avenue to integrated fiber technology. *Laser Photonics Rev.* **2012**, *6*, 709–723. [CrossRef]

23. Itoh, K.; Watanabe, W.; Nolte, S.; Schaffer, C.B. Ultrafast processes for bulk modification of transparent materials. *MRS Bull.* **2006**, *31*, 620–625. [CrossRef]

24. Chen, C.; Zhang, X.Y.; Yu, Y.S.; Wei, W.H.; Guo, Q.; Qin, L.; Ning, Y.Q.; Wang, L.J.; Sun, H.B. Femtosecond Laser-Inscribed High-Order Bragg Gratings in Large-Diameter Sapphire Fibers for High-Temperature and Strain Sensing. *J. Lightwave Technol.* **2018**, *36*, 3302–3308. [CrossRef]

25. Xu, X.Z.; He, J.; Liao, C.R.; Wang, P.P. Multi-layer, offset-coupled sapphire fiber Bragg gratings for high-temperature measurements. *Opt. Lett.* **2019**, *44*, 4211–4214. [CrossRef]

26. Grobnic, D.; Mihailov, S.J.; Ballato, J.; Dragic, P.D. Type I and II Bragg gratings made with infrared femtosecond radiation in high and low alumina content aluminosilicate optical fibers. *Optica* **2015**, *2*, 313–322. [CrossRef]

27. Zheng, Z.M.; Yu, Y.S.; Zhang, X.Y.; Guo, Q.; Sun, H.B. Femtosecond Laser Inscribed Small-Period Long-Period Fiber Gratings With Dual-Parameter Sensing. *IEEE Sens. J.* **2018**, *18*, 1100–1103. [CrossRef]